Physica E 144 (2022) 115469

Contents lists available at ScienceDirect

Physica E: Low-dimensional Systems and Nanostructures

journal homepage: www.elsevier.com/locate/physe

Optimizing the size and amount of CdS quantum dots for efficiency enhancement in CdS/N719 co-sensitized solar cells

M.A.K.L. Dissanayake [a,*], T. Jaseetharan [a,b], G.K.R. Senadeera [a,c], B.-E. Mellander [d], I. Albinsson [e], M. Furlani [d]

[a] National Institute of Fundamental Studies, Hantana Road, Kandy, Sri Lanka
[b] Department of Physical Sciences, South Eastern University of Sri Lanka, Sammanthurai, Sri Lanka
[c] Department of Physics, The Open University of Sri Lanka, Nawala, Nugegoda, Sri Lanka
[d] Department of Applied Physics, Chalmers University of Technology, Gothenburg, Sweden
[e] Department of Physics, University of Gothenburg, Gothenburg, Sweden

ARTICLE INFO

Keywords:
CdS quantum dots
SILAR method
N719 dye
ZnS layer
Co-sensitization
Multiple exciton generation
Energy gap

ABSTRACT

Co-sensitization of TiO_2 photoanodes in solar cells with Ruthenium dye and quantum dots offer better photovoltaic performance compared to the sensitization by the dye only. In the present study, TiO_2 nanostructured photoanode was co-sensitized with CdS quantum dots and N719 dye. CdS quantum dots were deposited using successive ionic layer adsorption and reaction (SILAR). A suitable thin ZnS interfacial layer has been introduced between two sensitizers to prevent the corrosion of CdS quantum dots by the iodide-based liquid electrolyte. In order to get the highest efficiency, the number of SILAR cycles for CdS quantum dot deposition has been optimized. A power conversion efficiency of 6.79% with short-circuit current density of 15.55 mA cm^{-2} and open circuit voltage of 764.5 mV have been obtained for the co-sensitized solar cell made with TiO_2/CdS/ZnS/N719 co-sensitized photoanode under the illumination of 100 mW cm^{-2} with AM 1.5 spectral filter. Efficiency and short-circuit current density of the solar cell have been enhanced by 11.31% and 6.58% respectively due to the co-sensitization. The optimized co-sensitized solar cell shows a higher incident photon to current conversion efficiency and a reduced electron recombination compared to the solar cell with dye-sensitized photoanode. Higher recombination resistance and longer electron lifetime of the solar cell with CdS/ZnS/N719 co-sensitized TiO_2 photoanode have contributed to the increased short circuit current and open circuit voltage leading to the enhanced efficiency of 6.79% which is among the highest for a co-sensitized dye sensitized solar cell.

1. Introduction

Dye-sensitized solar cells (DSSCs) are a promising class of devices for solar energy conversion applications. In these solar cells, Ruthenium-based dyes are commonly used to sensitize the TiO_2 photoanode. These dyes show broad absorption in the visible region of the solar spectrum. However, one dye molecule can create only one electron-hole pair from one photon whereas one semiconductor quantum dot can create more than one electron-hole pairs due to the ability of multiple exciton generation. Semiconductor quantum dots have attracted extensive attention over the past decades with different applications including light emitting diodes [1–3], photodetectors [4–6], transistors [7,8], spectrometers [9,10] and solar cells [11–13] due to their unique size dependent optoelectronic properties [14,15]. Quantum dot-sensitized solar cells have gained more attention in the area of solar energy conversion systems due to their low production cost and the excellent properties such as the ability of multiple exciton generation and high molar extinction coefficients [16–18]. Jing Li et al. reported dye-sensitized solar cells co-sensitized by CdS quantum dots and N719 with an efficiency of 5.57% [19]. Recently, co-sensitization of TiO_2 by PbS quantum dots and N719 has been reported with an efficiency of 6.35% by Yanqiong Liu et al. [20]. Subramaniam et al. reported CdSe quantum dots and N719 co-sensitized hierarchical TiO_2 nanorod based co-sensitized solar cell with an efficiency of 3.93% [21]. In another related study, Meng et al. [22] reported CdS/N719 co-sensitized solar cell with an efficiency of 3.93%. In addition to the CdS quantum dots, carbon quantum dots and doped quantum wells have been studied recently in the solar energy conversion process. $CsPb(Br_xI_{1-x})_3$ quantum

* Corresponding author.
E-mail address: lakshman.di@nifs.ac.lk (M.A.K.L. Dissanayake).

https://doi.org/10.1016/j.physe.2022.115469
Received 25 September 2021; Received in revised form 22 July 2022; Accepted 9 August 2022
Available online 21 August 2022

dots and $CsPb(Cl_xBr_{1-x})_3$ quantum dots show better photostability and absorption in ultraviolet region [23]. Haiguang Zhao et al. reported Cs_4PbBr_6 quantum dot based solar cells with a power conversion efficiency of 1.8% under the natural sun illumination (30 mW cm^{-2}) [24]. Haiguang Zhao et al. reported the eco-friendly and high efficiency solar concentrators with carbon quantum dots popularly known as "green quantum dots" [25]. Vertically aligned ZnO nanowires-based CdTe quantum dots and dye solar cells have been reported [26]. Recently, organic solar cell has been reported by Zhang et al. with simultaneously enhanced photocurrent and open circuit voltage medium-band gap acceptor [27]. Haung et al. reported the effect of ZnSe passivation layer on the performance of CdS/CdSe quantum dot sensitized solar cells [28]. High efficiency CdS/CdSe quantum dot-sensitized solar cells with two ZnSe layers with an efficiency of 7.24% [29].

Number of dye molecules on TiO_2 nanoporous electrode also determines the efficiency of the solar cell. Usually, monolayer of dye molecules is better to give high efficiency. If we increase the number of dye molecules, they form multilayers on the TiO_2 nanostructure. If we use another type of sensitizer with different absorption region, the performance of the cell can be enhanced. In the present study, TiO_2 photoanode nanostructure was co-sensitized with CdS quantum dots and N719 dye. In order to achieve a higher efficiency, the number of cycles used for deposition of CdS by SILAR method was optimized using I–V measurements on trial solar cells. Both, the iodide/triiodide redox couple as well as the polysulfide electrolyte is compatible with N719 dye and quantum dots. However, in the presence of the polysulfide electrolyte, regeneration of dye molecules is very poor. Therefore, iodide-based electrolytes are better to be used in co-sensitized solar cells. In this case, again, quantum dots are corroded by iodide electrolytes and a possible strategy to overcome this is to isolate the CdS quantum dots by a thin semiconductor layer of a different material, such as ZnS with a suitable thickness. By this way, we have been able to fabricate and characterize highly efficient, CdS/N719 co-sensitized solar cells.

Fig. 1 shows the schematic energy level diagram of TiO_2/CdS/ZnS/N719 co-sensitized photoanode. Conduction band of TiO_2 is slightly lower than that of CdS quantum dots which enables the efficient electron injection. Conduction band edge of CdS quantum dot is lower than the lowest unoccupied molecular orbit (LUMO) of N719 dye molecule. It can be seen that, the photo-generated electrons in N719 dye molecules can easily transferred to the conduction band of TiO_2. ZnS passivation layer prevents the electron transfer back reaction from the CdS quantum dots and TiO_2 photoanode to the electrolyte. Highest occupied molecular orbital (HOMO) of N719 dye is higher than the edge of the valence band of CdS and TiO_2. Therefore, N719 acts as a hole scavenger for the CdS

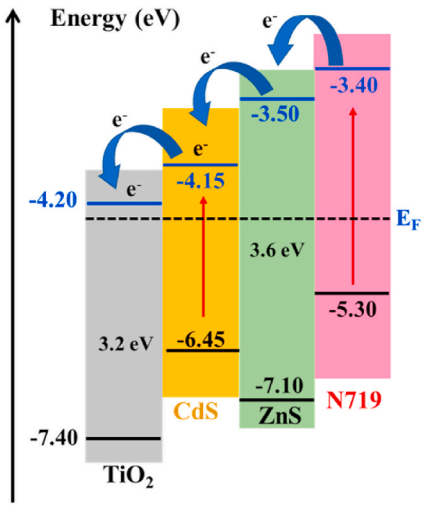

Fig. 1. Schematic energy level diagram of TiO_2/CdS/ZnS/N719 co-sensitized photoanode.

quantum dots in addition to the sensitization [30,31]. In this work, iodide-based redox couple was used as the electrolyte. In order to prevent the corrosion of CdS quantum dots, a narrow ZnS passivation layer was deposited between the CdS quantum dots and the N719 dye. In this study, ZnS deposition with 2 SILAR cycles gives the best efficiency for the CdS/ZnS/N719 co-sensitized solar cell. The presence of a narrow ZnS layer acts as a dielectric layer between the CdS layer and the N719 dye molecules and facilitate the effective charge transfer [31]. Optimized thickness of the ZnS passivation layer protects the CdS quantum dots from iodide-based electrolyte without affecting the photoinduced electron transfer.

2. Experimental

2.1. Materials

Fluorine-doped tin oxide (FTO) coated glass (8 Ω cm^{-2}, Solarnoix), Triton X-100 (Sigma-Aldrich), Titanium (IV) isopropoxide (97%, Fluka), Propan-1-ol (99.9%, Fisher), glacial acetic acid (99%, Fisher), Titanium dioxide P90 powder (Evonik), Titanium dioxide powder P25 (Degussa), Hydrochloric acid (37%, Sigma-Aldrich), Polyethylene glycol (99.8%, Sigma-Aldrich), *cis*-diisothiocyanato-bis(2,2′-bipyridyl-4,4′-dicarboxylato) ruthenium (II) bis (tetrabutylammonium) (N719 dye, Solaronix), Iodine (Sigma-Aldrich), Zinc acetate dihydrate (>99%, Sigma-Aldrich), Tetrapropylammonium iodide (≥98%, Sigma-Aldrich), Acetonitrile (99.8%, Sigma-Aldrich). Sodium sulfide hydrate (>60%, Sigma-Aldrich) and Cadmium (II) chloride (99.99%, Sigma-Aldrich) were used as received without any modification.

2.2. Preparation of TiO_2 electrode

0.25 g of TiO_2 P90 powder was ground for 15 min with 1 ml of 0.1 M HNO_3. The paste was spin coated on the conducting side of the FTO glass at 3000 rpm for 1 min and sintered at 450 °C for 45 min. For preparation of TiO_2 P25 paste, 0.25 g of TiO_2 powder and 1 ml of 0.1 M HNO_3 were ground. Then, 0.02 g of Triton X-100 and 0.05 g of Poly ethylene glycol 1000 were used as the binder and the mixture was ground until it became a creamy paste. This TiO_2 P25 paste was applied on TiO_2 P90 layer by doctor blade technique. Then the electrode was sintered at 450 °C for 45 min. The electrode was allowed to cool down to room temperature.

2.3. Preparation of TiO_2/CdS/ZnS/N719 photoanode structure

CdS quantum dots were incorporated on TiO_2 electrode by using SILAR technique. Aqueous solution of 0.1 M $CdCl_2$ and 0.1 M Na_2S were used as cationic and anionic precursor solutions respectively. In a SILAR cycle, dipping time in each solution was 1 min. Subsequently, the electrode was sintered at 120 °C for 10 min and allowed to cool. The number of SILAR cycles was optimized by using them in trial solar cells and checking their efficiency. The best CdS-sensitized TiO_2 electrode was dipped in to a 0.5 M aqueous solution of $Zn(CH_3COO)_2{\cdot}2H_2O$ for 1 min and then in a 0.5 M methanol solution of Na_2S for 1 min. Between each dipping, the electrode was rinsed into respective solvents. The number of SILAR cycle of ZnS passivation layer formation was optimized by using CdS/ZnS sensitized TiO_2 photoanodes in trial solar cells. Finally, CdS/ZnS quantum dot-sensitized TiO_2 electrodes were dipped in a 0.3 mM N719 dye solution and kept for 24 h for dye sensitization and subsequently washed with ethanol to remove excess of dye molecules.

2.4. Preparation of the redox electrolyte

Liquid iodide/triiodide redox couple was used as the electrolyte. To prepare this, 0.060 g of iodine, 0.738 g of tetrapropylammonium iodide and 3.6 ml of molten ethylene carbonate were mixed with 1 ml of acetonitrile and the mixture was stirred continuously for 12 h at room

temperature.

2.5. Optical absorption measurements

Optical absorption spectra of bare TiO_2 electrode, TiO_2/CdS photoanode, TiO_2/CdS/N719 photoanode, TiO_2/CdS/ZnS/N719 photoanode and N719 dye solution were obtained using Shimadzu 2450 spectrophotometer in the wavelength range from 350 nm to 1100 nm.

2.6. TEM and EDX analysis

Morphology and elemental composition of the CdS quantum dot-sensitized photoanodes with ZnS passivation layer were examined by using JEOL JEM-2100 High resolution transmission electron microscope (HRTEM) with an accelerating voltage of 200 kV. Energy dispersive X-ray (EDX) spectrum was obtained by using Ametek EDAX module with Octane T Optima-60 EDX detector in TEM mode.

2.7. Current – voltage characterization

CdS/ZnS/N719 co-sensitized TiO_2 photoanode and Pt coated counter electrode were assembled with coated sides facing each other using two gently pressed stainless-steel clips. I^-/I_3^- electrolyte solution was injected in to the space between the photoanode and the counter electrode to form a sandwich structure. Current-voltage measurements of each QDSSCs were made under the illumination of 100 mW cm^{-2} with AM 1.5 spectral filter using a computer-controlled multi-meter (Keithley 2000 model) coupled to a potentiostat/galvanostat unit (HA-301). The active area of the co-sensitized solar cell was 0.12 cm^2. Similarly, N719 dye-sensitized solar cell was characterized under the same conditions and used as the control device.

2.8. Electrochemical impedance spectroscopy (EIS) measurements

Electrochemical impedance spectra of solar cells fabricated using (a) N719 dye-sensitized TiO_2 photoanodes and (b) using CdS/ZnS/N719 co-sensitized TiO_2 photoanodes were obtained by using Autolab potentiostat/galvanostat PGSTAT128 N with FRA 32 M frequency response analyzer (Metrohm) under the illumination of 100 mW cm^{-2} with AM 1.5 spectral filter in the frequency range between 0.01 Hz and 1 MHz.

2.9. IPCE measurements

Incident photon to current conversion efficiency (IPCE) measurements of N719 dye-sensitized solar cells and CdS/N719 co-sensitized solar cells with and without ZnS layer were performed using Bentham PVE300 IPCE measurement system with TMc300 monochromator and Xenon arc lamp. Wavelength of the monochromator was varied between 300 nm and 1100 nm.

2.10. Stability tests

In this work, we studied the effect of co-sensitization using an acetonitrile based conventional liquid electrolyte without sealing and all solar cell measurements were taken immediately after assembling the cells. In this situation, after about 3 h, we observed that the efficiency reduced by about 30%. After 12 h efficiency reduced by 42%.

However, after the solar cell edges s were sealed with silicon glue, after 48 h, the efficiency was found to drop only by 0.5% from the initial value (as prepared). After this the, efficiency was reduced by about 12% after 15 days.

If we use better sealing methods with solvent electrolyte OR if we replaced the liquid electrolyte by quasi-solid (gel) electrolyte, we could have enhanced the stability further. However, in this study, our focus was only on the effect of co-sensitization.

3. Results and discussion

3.1. Optimization of CdS film deposition by SILAR method

Fig. 2 shows the optical absorption spectra of bare TiO_2 electrode and CdS quantum dot-sensitized TiO_2 electrodes with different number of SILAR cycles used for the optimization. Absorption increases with the number of SILAR cycles and the CdS quantum dot-sensitized TiO_2 electrodes shows a broad absorption between 450 and 550 nm and the absorption peaks shift towards the higher wavelength region with the number of SILAR cycles. It clearly shows that the size of the CdS quantum dots increases with the number of SILAR cycles similar to other quantum dots reported [32,33].

Fig. 3 shows $(Ah\nu)^2$ versus photon energy $(h\nu)$ plots. Here, A is the absorption coefficient of the photoanode material, h is the Planck's constant and ν is the frequency of the incident photon. Optical energy band gap of the CdS quantum dot sensitized TiO_2 electrodes decreases with the number of SILAR cycles due to the quantum confinement effect [34]. Calculated optical band gaps of CdS photoanodes extracted from the intersections of the straight lines are listed in Table 1.

As seen from Table 1, the optical energy bandgap of the TiO_2/CdS photoanodes decreases with the increasing number of CdS SILAR cycles. Absorption of the bare TiO_2 is in the ultraviolet region. After incorporation of CdS quantum dots, the absorption of the TiO_2 electrode is red shifted. Therefore, the optical bandgap of the TiO_2/CdS electrode has narrowed from 3.26 to 2.90 eV due to the incorporation of CdS quantum dots. This confirms the shifting of the absorption spectra towards long wavelengths with the number of SILAR cycles. In this study, the number of SILAR cycles was varied while the dipping times for each precursor solution were kept unchanged at 1 min. Jeong et al. [35] studied the size of the CdS quantum dots with SILAR adsorption time by fixing the number of SILAR cycles and changing the adsorption time. They have obtained the best photoanode corresponding to 30 min adsorption time and concluded that, more adsorption time will cause aggregation of CdS quantum dots. The amount and size of the CdS quantum dots have a significant impact on the photocurrent density and a suitable photoanode has been identified by current-voltage characterization of the fabricated CdS QDSSCs. In the present work, as shown in Fig. 8, the CdS quantum dot sensitized, TiO_2/CdS photoanode corresponding to 10 CdS SILAR cycles has shown the highest solar cell efficiency of 1.12%. However, as seen from Fig. 9, the CdS/N719 co-sensitized photoanode made with 6 SILAR cycles of CdS quantum dots shows the highest solar

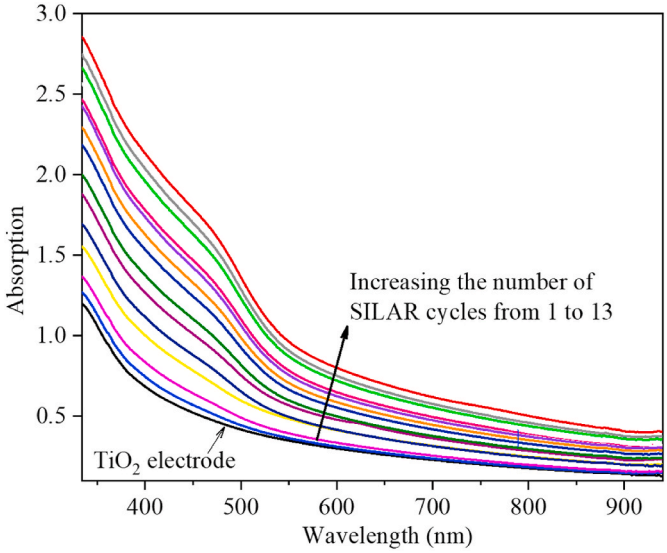

Fig. 2. Optical absorption of TiO_2 electrode and CdS quantum dot-sensitized TiO_2 electrodes.

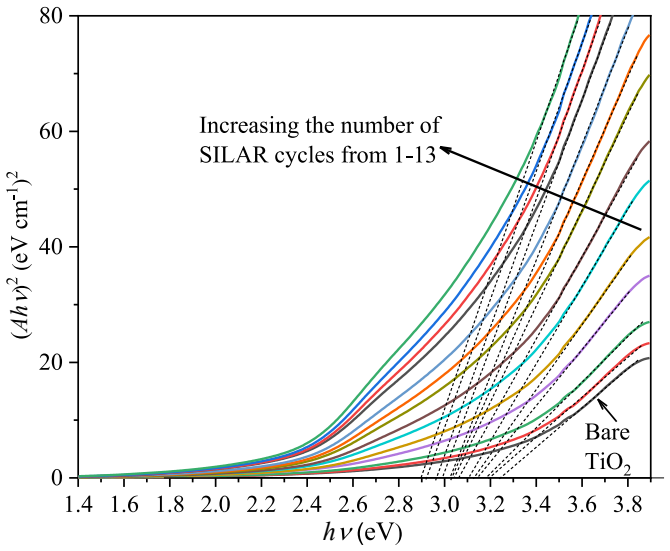

Fig. 3. $(Ah\nu)^2$ versus photon energy $(h\nu)$ plots of CdS quantum dot-sensitized TiO_2 electrodes.

Table 1
Variation of estimated optical energy gaps of photoanodes with different CdS SILAR cycles.

Photoanode	Optical energy gap (eV)	Photoanode	Optical energy gap (eV)
TiO_2	3.26	TiO_2/CdS (7)	3.05
TiO_2/CdS (1)	3.18	TiO_2/CdS (8)	3.04
TiO_2/CdS (2)	3.17	TiO_2/CdS (9)	3.02
TiO_2/CdS (3)	3.14	TiO_2/CdS (10)	2.99
TiO_2/CdS (4)	3.12	TiO_2/CdS (11)	2.96
TiO_2/CdS (5)	3.10	TiO_2/CdS (12)	2.92
TiO_2/CdS (6)	3.06	TiO_2/CdS (13)	2.90

cell efficiency.

3.2. TEM and EDX analysis

Fig. 4 shows the TEM image of CdS quantum dot-sensitized TiO_2/CdS electrode made with 6 CdS SILAR cycles covered with a ZnS passivation layer. This number of SILAR cycles for co-sensitization with N719 dye was optimized by current-voltage characterization of solar cells fabricated with TiO_2/CdS/ZnS photoanode. The size of the CdS quantum dots

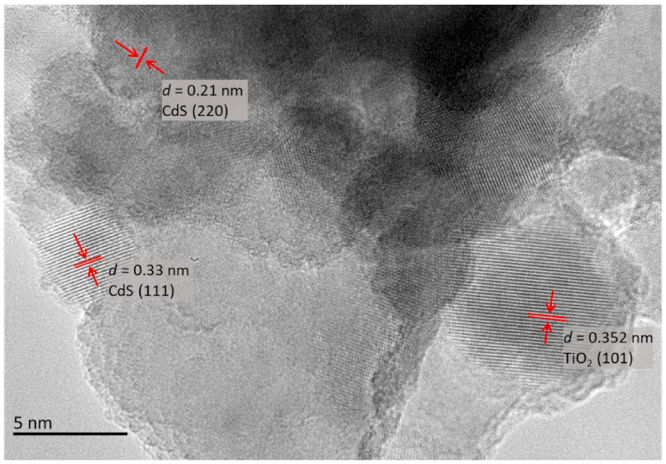

Fig. 4. TEM image of CdS quantum dot-sensitized TiO_2 electrode.

is in the range between 4.0 and 4.5 nm. ZnS passivation layer also can be seen in the TEM image. Presence of ZnS is further confirmed by EDX analysis.

Fig. 5 shows the EDX spectrum of CdS quantum dot-sensitized TiO_2 electrode with ZnS passivation layer labeled as TiO_2/CdS/ZnS electrode. This EDX spectrum confirms the presence of Cd, Zn and S in the TiO_2 electrode.

3.3. Optical absorption of N719 dye solution

Fig. 6 shows the optical absorption spectrum of N719 dye solution which shows the main absorption peaks around 525 nm in the mid-visible region.

Fig. 7 shows the optical absorption spectra of bare TiO_2 photoanode, TiO_2/CdS photoanode, TiO_2/CdS/N719 co-sensitized photoanode and TiO_2/CdS/ZnS/N719 co-sensitized photoanode. From this figure, it is clear that the TiO_2 photoanode, co sensitized with CdS Q-dots and the N719 dye has significantly enhanced the optical absorption of the photoanode in the wavelength range between 420 and 550 nm. Introduction of the ZnS passivation layer shows only a marginal increase of optical absorption on this region.

3.4. Optimization of CdS film thickness

Appropriate size and amount of CdS quantum dots in co-sensitized TiO_2 electrode play a major role in the efficiency of the solar cells. Fig. 8 displays the variation of SILAR cycle number on the efficiency of CdS QDSSCs. With the incorporation of CdS Q-dots, efficiency of the CdS QDSSCs gradually increases with number of SILAR cycles up to a maximum value of 1.12% corresponding to 10 SILAR cycles. In this range, the amount and size of the quantum dots incorporated in the photoanode increase with number of SILAR cycles which enhances the photon absorption thereby increasing the performance of the solar cells. However, when the number of SILAR cycles increased beyond 10, the efficiency decreases. This could be due to the agglomeration of small size CdS to form bigger particles limiting the contact area for redox species of the electrolyte with the photoanode. Due to this, photoelectron transfer and regeneration of the quantum dots are affected. Aggregation of quantum dots and can also weaken the average electronic coupling and increase the average distance between the quantum dots and TiO_2 nanostructure [36–39].

Fig. 9 shows the efficiency of the TiO_2/CdS/N719 co-sensitized solar cells with the number of SILAR cycles for CdS deposition. Efficiency of the co-sensitized solar cell gradually increases almost linearly with the number of SILAR cycles and exhibits the maximum efficiency of 6.73% corresponding to 6 SILAR cycles. Beyond the 6 SILAR cycles, the efficiency decreases quite similar to the mechanism described earlier.

In the TiO_2/CdS/N719 photoanode also increasing the number of CdS SILAR cycles leads to an increase in the size of the quantum dots which affects the average separation between the quantum dots and the TiO_2 nanostructure while the increase in the number of quantum dots lead to an aggregation and reduces the performance of the solar cell [36, 37]. This feature is clearly shown schematically in Fig. 10(b). When the SILAR cycle number is increased to 6 and above, it will increase the number as well as the particle size of CdS quantum dots in the TiO_2 photoanode, which, when dipped in the N719 dye solution, will clog the pores of TiO_2 nanoporous structure. This will limit the diffusion of the electrolyte into TiO_2 pores, leading to a higher recombination of photoexcited electrons, and reducing the short-circuit current density as described also by Li et al. [30]. According to them, the excessive CdS quantum dots can act as a kind of recombination center instead of providing a favorable electron transfer.

3.5. Incorporation of ZnS passivation layer

Fig. 11 shows the efficiency variation of the co-sensitized solar cells

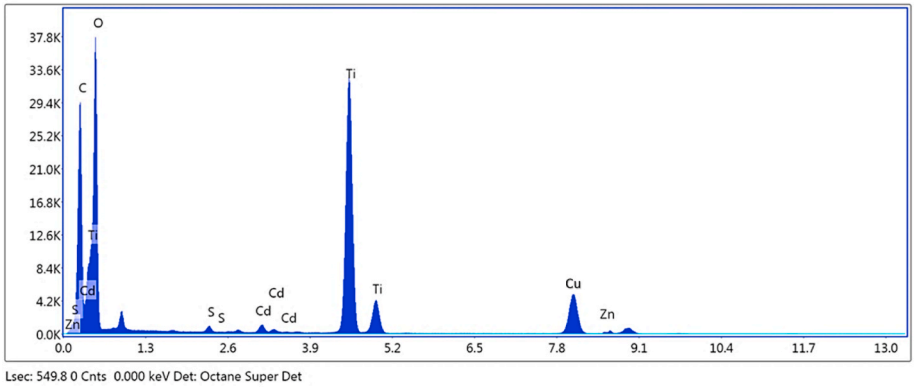

Fig. 5. EDX spectrum of TiO_2/CdS/ZnS electrode.

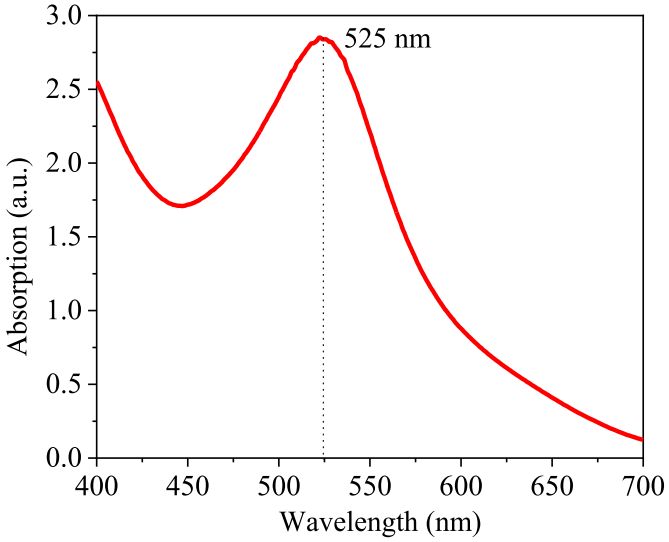

Fig. 6. Optical absorption spectrum of N719 dye solution.

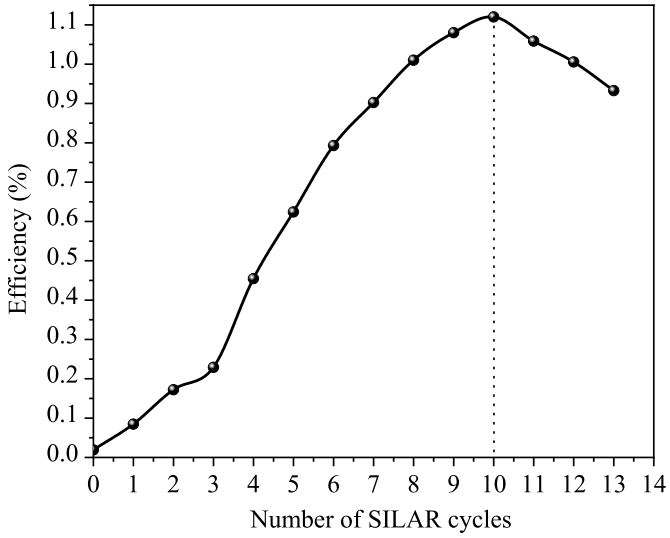

Fig. 8. Variation of efficiency of TiO_2/CdS QDSSCs with number of CdS SILAR cycles.

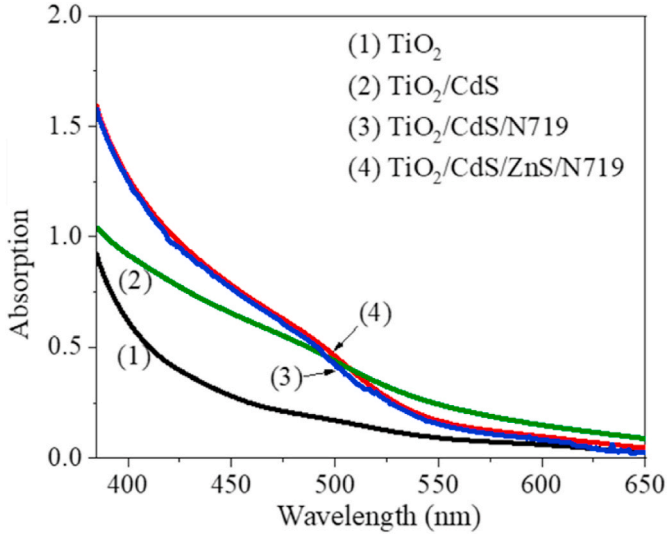

Fig. 7. Optical absorption spectra of (1) bare TiO_2 electrode, (2) TiO_2/CdS photoanode, (3) TiO_2/CdS/N719 photoanode and (4) TiO_2/CdS/ZnS/N719 photoanode.

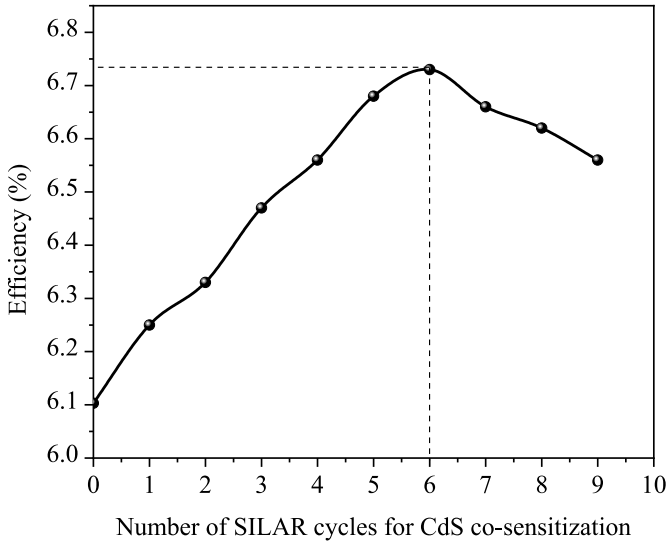

Fig. 9. Efficiency variation of TiO_2/CdS/N719 co-sensitized solar cells with the number of CdS SILAR cycles.

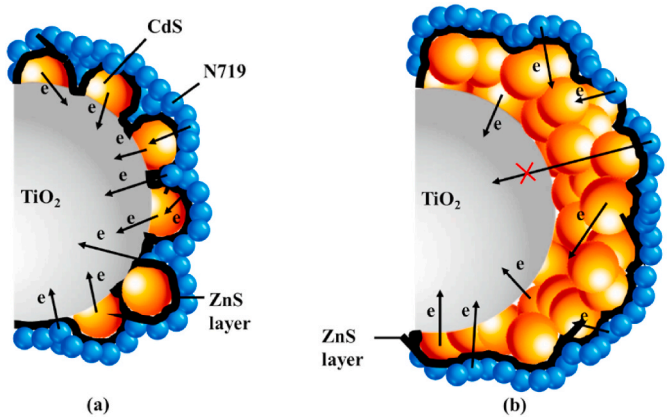

Fig. 10. Effect of quantum dot aggregation on the electron transfer (a) no aggregation of CdS quantum dots (b) more aggregation of CdS quantum dots.

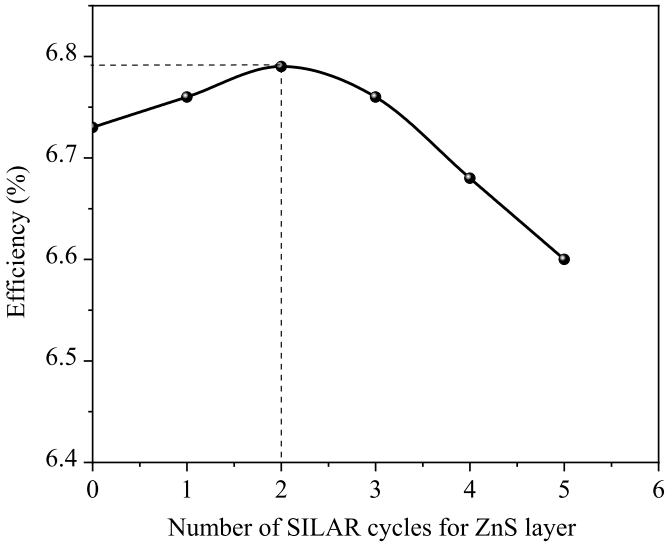

Fig. 11. Efficiency variation of CdS/ZnS/N719 co-sensitized solar cells with the number of ZnS SILAR cycles.

with the number of SILAR cycles for ZnS interfacial layer deposition. Efficiency of the solar cell gradually increases with the number of SILAR cycles and show a maximum value of 6.79% corresponding to 2 cycles. In the presence of a narrow ZnS passivation layer, the photostability of the CdS quantum dots has been improved by preventing the chemical corrosion from the iodide electrolyte without affecting the photoinduced charge transfer process. Beyond the two SILAR cycles, the efficiency gradually decreases. Thicker ZnS layer reduces the photoelectron transfer.

3.6. Photovoltaic performance comparison

Fig. 12 shows the current-voltage characteristics of N719 dye-sensitized solar cell and CdS/ZnS/N719 dye co-sensitized solar cell. Co-sensitized solar cell shows a higher short-circuit current density due to the efficient absorption and charge carrier injection to the TiO_2 conduction band. Photovoltaic parameters are summarized in Table 2.

The best co-sensitized solar cell shows an efficiency of 6.79% with a highest short-circuit current density of 15.55 mA cm^{-2}. The corresponding solar cell sensitized only with N719 dye shows an efficiency of 6.10% under the same illuminating conditions. Enhancements of 11.31% in efficiency and 12.11% in current density have been achieved due to the co-sensitization of the DSSCs by the dye and CdS quantum dots.

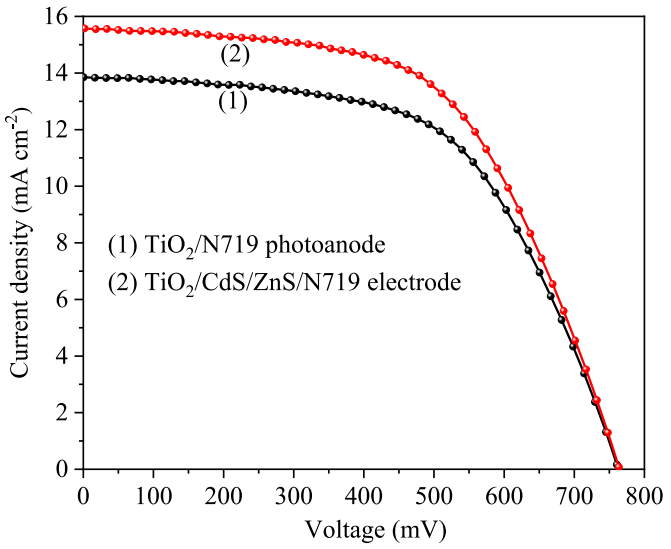

Fig. 12. Current-voltage characterization of dye-sensitized solar cell and CdS Q-dot/dye co-sensitized solar cell under the simulated light of 100 mW cm^{-2} with AM 1.5 spectral filter.

Table 2
Photovoltaic parameters of the dye sensitized and co-sensitized solar cells under the illumination of 100 mW cm^{-2}

Sensitizers	J_{SC} (mA cm^{-2})	V_{OC} (mV)	*FF* (%)	Efficiency (%)
N719 dye	14.59	762.10	57.75	6.10
CdS/ZnS/N719 dye	15.55	764.50	57.13	6.79

dots.

3.7. IPCE measurements

Fig. 13 shows the IPCE curves of CdS quantum dot-sensitized solar cell, N719 dye-sensitized solar cell, CdS/N719 co-sensitized solar cell and CdS/ZnS/N719 co-sensitized solar cell with ZnS layer. Estimated IPCE values are 47.3%, 56.1%, 57.0 and 59.5% respectively. CdS QDSSC shows a broad peak around between 450 and 500 nm which corresponds to the strong absorption of CdS quantum dots (Fig. 7). Similarly, DSSC

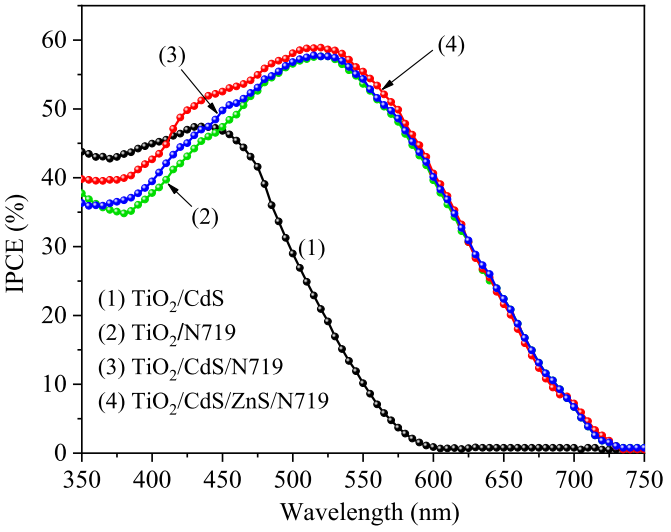

Fig. 13. IPCE curves of CdS QDSSC, N719 dye-sensitized solar cell, CdS/N719 dye co-sensitized solar cells with and without ZnS coating.

shows a broad peak between 450 and 650 nm which corresponds to the absorption of the N719 dye (Fig. 6). There is no significant enhancement in the maximum value of the IPCE due to the co-sensitization. However, the spectral response range of CdS/ZnS/N719 co-sensitized solar cell is wider than N719 dye-sensitized solar cell. IPCE depends on light harvesting efficiency, charge injection efficiency and charge collection efficiency [40]. Optimized amount and size of CdS quantum dots and dye in the photoanode enhances the light absorption and the suitable band alignment of quantum dot and N719 dye enhances the efficient charge injection.

3.8. Analysis of EIS spectra

Electrochemical parameters of the best N719 based dye-sensitized solar cell and the best CdS/ZnS/N719 co-sensitized solar cell were extracted by fitting suitable equivalent circuits to the Nyquist plots as shown in Fig. 14. Fig. 15 shows the corresponding Bode phase plots of the two solar cell types. CPE_1 and CPE_2 are the constant phase elements. R_S is the series resistance which represents the FTO/TiO_2 interface, R_{1CT} is the resistance at the counter electrode/electrolyte interface and R_{2CT} is the resistance at the photoanode/electrolyte interface which is known as the recombination resistance. W is the finite Warburg impedance element.

Fig. 15 shows the Bode phase plots of N719 dye-sensitized solar cell and CdS/N719 co-sensitized solar cell. Estimated interface resistances and electron lifetimes of the solar cells are listed in Table 3.

There is no significant change in the series resistance R_s between the two solar cells. However, the CdS/ZnS/N719 co-sensitized solar cell shows a lower charge transfer resistance (R_{1CT}) and a high recombination resistance (R_{2CT}) compared to the N719 DSSC. This indicates that the recombination of the electrons in the co-sensitized photoanode and the electrolyte has reduced. It has been reported that a TiO_2 atomic layer deposition between CdS QDs and the dye of a quantum dot and dye co-sensitized solar cells can enhance the performance by reducing the interfacial recombination of electrons [43,44]. The increase in J_{sc} in the CdS QD sensitized solar cell with ZnS layer between the CdS QD and N719 dye molecules in the present work also appears to be due to the cumulative effect of low charge transfer resistance R_{1CT} and low charge recombination rate.

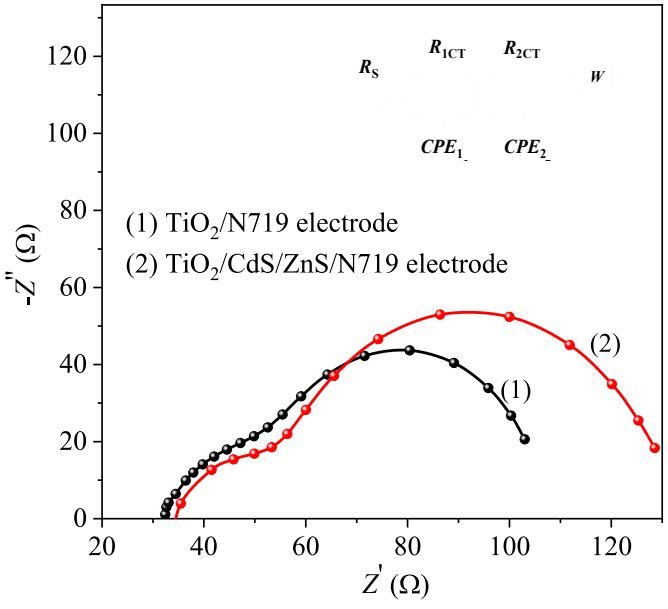

Fig. 14. Nyquist plots of the N719 dye-sensitized solar cell and the CdS/ZnS/N719 co-sensitized solar cell measured under the intensity of 100 mW cm^{-2} with AM 1.5 filter.

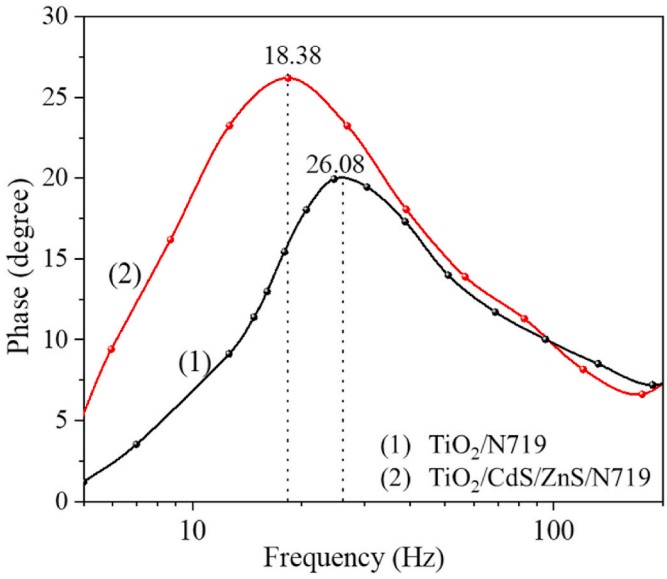

Fig. 15. Bode phase of the N719 dye-sensitized solar cell and the CdS/ZnS/N719 co-sensitized solar cell extracted from the EIS spectra shown in Fig. 13.

Table 3
Electrochemical impedance parameters of the N719 dye-sensitized solar cell and the CdS/ZnS/N719 co-sensitized solar cell obtained from fitting the data to the equivalent circuits shown in Fig. 13 using Nova software.

Sensitizer	R_S (Ω)	R_{1CT} (Ω)	R_{2CT} (Ω)	τ (ms)	J_{sc} (mA cm^{-2})	Efficiency (%)
N719 dye	32.5	41.3	52.3	6.1	14.6	6.10
CdS/ZnS/ N719 dye	34.2	32.8	71.4	8.6	15.6	6.79

R_{2CT} represents the charge transfer resistance at the TiO_2/Quantum dots/electrolyte interface within the TiO_2 photoanode which corresponds to the second and large semicircle in the Nyquist plot. Because R_{2CT} represents the charge recombination resistance, the higher the value of R_{2CT}, it is harder for the photogenerated electrons in the photoanode to recombine with the electrolyte redox couple leading to a decrease in the charge recombination rate. The electron lifetime is longer for the cell with CdS/ZnS/N719 co-sensitized TiO_2 photoanode than that of the cell with TiO_2 photoanode without ZnS passivation layer. This clearly suggests that the CdS/ZnS/N719 co-sensitized TiO_2 photoanode with the ZnS passivation layer has prolonged the electron lifetime leading to reduced charge recombination at the TiO_2/CdS/ZnS/N719 photoanode-electrolyte interface. Reduced interface charge recombination also contributes to a higher V_{oc} as observed in the present case (Table 2). These results confirms that fact that the Q-dots/dye co-sensitization facilitates effective electrons transfer with less recombination resulting in a higher short-circuit photo current [41,42].

3.9. Stability tests

In this work, we studied the effect of co-sensitization using an acetonitrile based conventional liquid electrolyte without sealing and all solar cell measurements were taken immediately after assembling the cells. In this situation, after about 3 h, we observed that the efficiency reduced by about 30%. After 12 h efficiency reduced by 42%. However, after the solar cell edges were sealed with silicon glue, after 48 h, the efficiency was found to drop only by 0.5% from the initial value (as prepared). After this the efficiency was reduced by about 12% after 15 days. All our measurements used for solar cell characterization were done for "as fabricated" solar cells as the focus of this study was to study

the effect of co-sensitization.

4. Conclusion

CdS/N719 dye co-sensitized solar cells along with a ZnS layer between the CdS Q-dots and the N719 dye molecules were fabricated and characterized with optimized amount of CdS quantum dots and N719 dyes in the TiO_2 photoanode. It shows a maximum efficiency of 6.79% corresponding to 6 CdS SILAR cycles and 2 ZnS SILAR cycles. The results demonstrate that the CdS Q-dot/N719 dye along with ZnS interfacial layer can significantly improve the short circuit current density of the solar cell and enhance the energy conversion efficiency while also improving the stability of the CdS Q-dots against reactions with redox electrolyte. This structure also reduces the photo-excited electron recombination with the electrolyte while reducing the internal resistance as confirmed by optical absorption, *I–V,* IPCE and EIS measurements. The optimized co-sensitized solar cell shows an efficiency of 6.79% with a higher short-circuit current density of 15.55 mA cm^{-2}. The corresponding solar cell sensitized only with N719 dye shows an efficiency of 6.10%.

Ethical statement

On behalf of all the authors of this manuscript, I wish to confirm that:

- The manuscript or any of its parts have not been submitted to any other journal for simultaneous consideration.
- The submitted work is original and have not been published elsewhere in any form or language (partially or in full).

Declaration of competing interest

The authors declare that they have no known competing financial interests or personal relationships that could have appeared to influence the work reported in this paper.

Data availability

No data was used for the research described in the article.

Acknowledgments

The Authors gratefully acknowledge the financial support from the National Science Foundation, Sri Lanka under the grant number NSF/SCH/2018/04.

References

[1] W. Mei1, Z. Zhang, A. Zhang, D. Li, X. Zhang, H. Wang, Z. Chen, W. Li, X. Li, X. Xu, High-resolution, full-color quantum dot light-emitting diode display fabricated via photolithography approach, Nano Res. 13 (2020) 2485–2491.
[2] F. Chen, Q. Lin, H. Shen, A. Tang, Blue quantum dots-based electroluminescent light-emitting diodes, Mater. Chem. Front. 4 (2020) 1340–1365.
[3] K.P. Acharya, A. Titov, J. Hyvonen, C. Wang, J. Tokarz, P.H. Holloway, High efficiency quantum dot light emitting diodes from positive aging, Nanoscale 9 (2017) 14451–14457.
[4] A.D. Iacovo1, C. Venettacci, C. Giansante, L. Colace, Narrowband colloidal quantum dot photodetectors for wavelength measurement applications, Nanoscale 12 (2020) 10044–10050.
[5] H. Jeong, J.H. Song, S. Jeong, W.S. Chang, Graphene/PbS quantum dot hybrid structure for application in near-infrared photodetectors, Sci. Rep. 10 (2020), 12475.
[6] A. Yakimov, V. Kirienko, A. Bloshkin, A. Dvurechenskii, D. Utkin, Quantum dot based mid-infrared photodetector enhanced by a hybrid metal-dielectric optical antenna, J. Phys. D Appl. Phys. 53 (2020), 335105.
[7] F. Hetsch, N. Zhao, S.V. Kershaw, A.L. Rogach, Quantum dot field effect transistors, Mater. Today 16 (9) (2013) 312–325.
[8] S. Ihara, A. Andreev, D.A. Williams, T. Kodera, S. Oda, Quantum dots in single electron transistors with ultrathin silicon-on-insulator structures, Appl. Phys. Lett. 107 (2015), 013102.
[9] J. Bao, M.G. Bawendi, A colloidal quantum dot spectrometer, Nature 523 (2015) 67–70.
[10] X. Zhu, L. Bian, H. Fu, L. Wang, B. Zou, Q. Dai, J. Zhang, H. Zhong, Broadband perovskite quantum dot spectrometer beyond human visual resolution, Light, Science & App. 9 (2020) 73.
[11] A.J. Nozik, Quantum dot solar cells, Physica E 14 (2002) 115–120.
[12] S. Emin, S.P. Singh, L. Han, N. Satoh, A. Islam, Colloidal quantum dot solar cells, Sol. Energy 85 (2011) 1264–1282.
[13] V. Aroutiounian, S. Petrosyan, A. Khachatryan, K. Touryan, Quantum dot solar cells, J. Appl. Phys. 89 (2001) 2268.
[14] J. Melville, Optical Properties of Quantum Dots, UC Berkeley College of Chemistry, California, 2015.
[15] A. Credi, Photoactive Semiconductor Nanocrystal Quantum Dots, e-Book, Springer, 2019.
[16] A.J. Nozik, Multiple exciton generation in semiconductor quantum dots, J. Chem. Phy. Lett. 457 (2008) 3–11.
[17] C. Smith, D. Binks, Multiple exciton generation in colloidal nanocrystals, Nanomaterials 4 (2014) 19–45.
[18] W.W. Yu, L. Qu, W. Guo, X. Peng, Experimental determination of the extinction coefficient of CdTe, CdSe, and CdS nanocrystals, Chem. Mater. 15 (2003) 2854–2860.
[19] J. Li, L. Zhao, S. Wanga, J. Hu, B. Dong, H. Lu, L. Wana, P. Wang, Great improvement of photoelectric property from co-sensitization of TiO_2 electrodes with CdS quantum dots and dye N719 in dye-sensitized solar cells, Mater. Res. Bull. 48 (2013) 2566–2570.
[20] Y. Liu, J. Wang, Co-sensitization of TiO_2 by PbS quantum dots and dye N719 in dye-sensitized solar cells, Thin Solid Films 518 (2010) 54–56.
[21] M.R. Subramaniam, D. Kumaresan, CdSe quantum dots and N719-dye decorated hierarchical TiO_2 nanorods for the construction of efficient Co- sensitized solar cells, ChemPhysChem 16 (2015) 2543–2548.
[22] K. Meng, P.K. Surolia, O. Byrne, K.R. Thampi, Quantum dot and quantum dot-dye co-sensitized solar cells containing organic thiolate-disulfide redox electrolyte, J. Power Sources 275 (2015) 681–687.
[23] H. Zhaoa, D. Benetti, X. Tong, H. Zhang, Y. Zhou, G. Liu, D. Ma, S. Sun, Z.M. Wang, Y. Wang, F. Rosei, Efficient and stable tandem luminescent solar concentrators based on carbon dots and perovskite quantum dots, Nano Energy 50 (2018) 756–765.
[24] H. Zhao, R. Sun, Z. Wang, K. Fu, X. Hu, Y. Zhang, Zero-dimensional perovskite nanocrystals for efficient luminescent solar concentrators, Adv. Funct. Mater. 29 (2019), 1902262.
[25] H. Zhao, G. Liu, S. You, F.V.A. Camargo, M. Zavelani-Rossi, X. Wang, C. Sun, B. Liu, Y. Zhang, G. Han, A. Vomiero, X. Gong, Gram-scale synthesis of carbon quantum dots with large Stokes shift enables fabrication of eco-friendly and high-efficiency luminescent solar concentrators, Energy Environ. Sci. 14 (2021) 396–406.
[26] Z.H. Chen, C.P. Liu, H.E. Wang, Y.B. Tang, Z.T. Liu, W.J. Zhang, S.T. Lee, J. A. Zapien, I. Bello, Electronic structure at the interfaces of vertically aligned zinc oxide nanowires and sensitizing layers in photochemical solar cells, J. Phys. D Appl. Phys. 44 (2011), 325108.
[27] M. Zhang, M. Zeng, X. Deng, Z. Zhou, X. Tan, S. Tan, B. Zhao, J. Zhang, Y. Zou, Simultaneously enhancing the J_{sc} and V_{oc} of ternary organic solar cells by incorporating a medium-band-gap acceptor, ACS Appl. Energy Mater. 4 (2021) 43480–43486.
[28] F. Huang, J. Hou, H. Wang, H. Tang, Z. Liu, L. Zhang, Q. Zhang, S. Peng, J. Liu, G. Cao, Impacts of surface or interface chemistry of ZnSe passivation layer on the performance of CdS/CdSe quantum dot sensitized solar cells, Nano Energy 32 (2017) 433–440.
[29] F. Huang, L. Zhang, Q. Zhang, J. Hou, H. Wang, H. Wang, S. Peng, J. Liu, G. Cao, High Efficiency CdS/CdSe Quantum Dot Sensitized Solar Cells with Two ZnSe Layers, ACS Appl. Mater. Interfaces 8 (50) (2016) 34482–34489.
[30] J. Li, L. Zhao, S. Wang, J. Hu, B. Dong, H. Lu, L. Wan, P. Wang, Great improvement of photoelectric property from co-sensitization of TiO_2 electrodes with CdS quantum dots and dye N719 in dye-sensitized solar cells, Mater. Res. Bull. 48 (2013) 2566–2570.
[31] S. Luo, H. Shen, W. Hu, Z. Yao, J. Li, D. Oron, N. Wang, H. Lin, Improved charge separation and transport efficiency in panchromatic sensitized solar cells with co-sensitization of PbS/CdS/ZnS quantum dots and dye molecules, RSC Adv. 6 (2016) 21156–21164.
[32] R. Ahmed, G. Will, J. Bell, H. Wang, Size-dependent photodegradation of CdS particles deposited onto TiO_2 mesoporous films by SILAR method, J. Nano Res. 14 (2012) 1140.
[33] M. Nam, J. Park, S.-W. Kim, K. Lee, Broadband-absorbing hybrid solar cells with efficiency greater than 3% based on a bulk heterojunction of PbS quantum dots and a low-bandgap polymer, J. Math. Chem. A 2 (2014) 3978–3985.
[34] C. Cheng, J. Li, X. Cheng, Photoluminescence lifetime and absorption spectrum of PbS nanocrystal quantum dots, J. Lumin. 188 (2017) 252–257.
[35] M.-S. Jeong, M.-K. Son, S.-K. Kim, S. Park, K. Prabakar, H.-J. Kim, Study on characteristics of CdS quantum dot-sensitized solar cells prepared by Successive Ionic Layer Adsorption and Reaction with different adsorption times, Electron. Mater. Lett. 10 (3) (2014) 621–626.
[36] N. Guijarro, T. Lana-Villarreal, Q. Shen, T. Toyoda, R. Gomez, Sensitization of titanium dioxide photoanodes with cadmium selenide quantum dots prepared by SILAR: photoelectrochemical and carrier dynamics studies, J. Phys. Chem. C 114 (2010) 21928–21937.
[37] Y. Wang, Z. Li, F. Li, Y. Tian, W. Zhao, X. Liu, J. Yang, A Novel method for the preparation of CdS quantum dots sensitized solar cells based on free-standing and

through-hole TiO_2 nanotube arrays, J. Nanosci. Nanotechnol. 16 (2016) 6086–6092.

[38] S.K. Kokate, A.T. Supekar, P.K. Baviskar, B.M. Palve, S.R. Jadkar, K.C. Mohite, H. M. Pathan, CdS sensitized pristine and Cd doped ZnO solar cells: effect of SILAR cycles on optical properties and efficiency, Mater. Sci. Semicond. Process. 80 (2018) 179–183.

[39] K. Veerathangam, M.S. Pandian, P. Ramasamy, Influence of SILAR deposition cycles in CdS quantum dot-sensitized solar cells, J. Mater. Sci. Mater. Electron. 29 (2018) 7318–7324.

[40] Z. Chen, T.G. Deutsch, H.N. Dinh, K. Domen, K. Emery, A.J. Forman, N. Gaillard, R. Garland, C. Heske, T.F. Jaramillo, A. Kleiman-Shwarsctein, E. Miller, K. Takanabe, J. Turner, Incident photon-to-current efficiency and photocurrent spectroscopy, in: Photoelectrochemical Water Splitting, Springer, 2013, pp. 87–97.

[41] D. Punnoose, S.S. Rao, S.-K. Kim, H.-J. Kim, Exploring the effect of manganese in lead sulfide quantum dot sensitized solar cell to enhance the photovoltaic performance, RSC Adv. 5 (2015) 33136–33145.

[42] J. Tian, L. Lv, C. Fei, Y. Wang, X. Liu, G. Cao, A highly efficient (>6%) $Cd_{1-x}Mn_xSe$ quantum dot sensitized solar cell, J. Mater. Chem. 2 (2014) 19653–19659.

[43] Xiu Lin, Kehan Yu, Ganhua Lu, Junhong Chen, Chris Yuan, Atomic layer deposition of TiO_2 interfacial layer for enhancing performance of quantum dot and dye co-sensitized solar cells, J. Phys. D Appl. Phys. 46 (2013), 024004, https://doi.org/10.1088/0022-3727/46/2/024004.

[44] Wei Zheng, Xu Zhang, The improved performance of solar cells Co-sensitized with CdS/Ag2S quantum dots and N719 dye, J. Alloys Compd. (2021), https://doi.org/10.1016/j.jallcom.2021.161331.